This article has been accepted for inclusion in a future issue of this journal. Content is final as presented, with the exception of pagination.

Peer-Reviewed Technical Communication

Simulation-Driven Optimization of Underwater Docking Station Design

Brian R. Page and Nina Mahmoudian

***Abstract*—This paper presents the optimization of a novel docking design for docking and charging of autonomous underwater vehicles. The docking design has been optimized to maximize the capture envelope and minimize the maximum contact force. Two design parameters, sweep angle and ramp angle, were optimized as was the velocity during terminal homing and capture. The optimization was an exhaustive optimization with 5600 unique simulations completed that included the vehicle hydrodynamics, impact dynamics, and controller. Unique to the presented docking design is the ability to support a wide variety of vehicles from different size classes through its simplified funnel design and use of a docking adapter as validated in simulation with a Dolphin II AUV and Bluefin SandShark. The only part of the docking system that contacts the vehicle is a standardized docking adapter that is meant as a drop-in replacement for an antenna mast. The presented docking system is low-cost, compact, and can be deployed in a wide variety of situations including mobile docking.**

***Index Terms*—Autonomous underwater vehicle (AUV), charging, docking, marine robotics, optimization.**

I. Introduction

AUTONOMOUS underwater vehicles (AUVs) have seen rapidly expanding usage over the past decade with advances in computation, miniaturization, sensors, and energy storage. Modern AUVs are able to explore the deepest depths of the world's oceans and collect a wide assortment of useful information for commercial, military, and scientific missions. These AUVs are however limited in endurance due to the restricted energy storage capacities of current battery technology. With these limitations, typical AUV endurance is approximately one day with a manual retrieval and recharging process required between missions. The manual retrieval and recharging process necessitates a manned surface vessel to support the AUV, dramatically increasing costs. In open ocean, manned surface vessel costs are in excess of $30 000 per day [1], [2]. Despite the large costs, extended AUV missions do occur such as mine detection [3], [4], Arctic studies [5], [6], and marine geoscience [7].

One proposed solution to the endurance limitation of AUVs is automated underwater charging stations [8]– [10]. These charging stations can be equipped with sources of power either through renewables (solar, wind, wave) or shore power meaning that they can support charging AUVs indefinitely. Using existing technology, some AUVs are able to operate for extended periods away from manned surface vessels [11]. These existing stations however are limited in their adaptability to other platforms, are costly to install, and are unable to be modified for mobile applications. Additionally, the infrastructure to support persistence is fixed, which is not suitable for transient or expansive missions.

Manuscript received October 5, 2017; revised May 7, 2018 and September 30, 2018; accepted November 29, 2018. This work was supported in part by the National Science Foundation under Grant 1453886 and in part by the Office of Naval Research N00014-15-1-2599. *(Corresponding author: Nina Mahmoudian.)*

Associate Editor: F. Zhang.

The authors are with the Department of Mechanical Engineering–Engineering Mechanics, Michigan Technological University, Houghton, MI 49931 USA, and also with Purdue University, West Lafayette, IN 47907 USA (e-mail: bpage@mtu.edu; page82@purdue.edu; ninam@mtu.edu; ninam@purdue.edu).

Digital Object Identifier 10.1109/JOE.2018.2885200

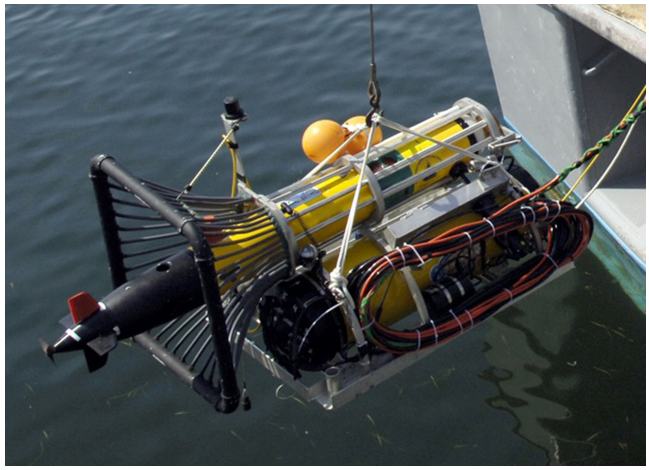

Fig. 1. REMUS docking station being deployed during AUV Fest 2007. Image courtesy of US Navy with ID 070611-N-7676W-023.

In this paper, we present a low-cost, adaptable AUV docking station that utilizes a novel capture design. The design features a large capture envelope and is adaptable to support the vast majority of modern traditional AUVs. Additionally, the docking station is designed so that it can be developed to serve as a mobile charging station.

The remainder of this paper provides a background in Section II, a detailed description of the novel docking station in Section III, the dynamic modeling of the docking maneuver in Section IV, simulation results in Section V, and finishes with a brief conclusion and future work in Section VI.

II. Background

Docking stations for AUVs traditionally consist one of two types: a large cone shaped funnel [8], [9], [12], [13] or a pole [11] and are compared extensively in [2] and [14]. By far the most common docking technique is the cone shaped funnel [14]. In this style of docking station, a large funnel is installed on either the seafloor or any other large system such as on a much larger AUV [15]. The docking procedure for funnel designs involves the AUV homing into the funnel and being guided in by bouncing off of and sliding along the funnel face. Once inside of the funnel, the AUV is latched and power transfer is begun. To undock, the AUV uses reverse thrust until at a safe distance away before resuming the mission. Funnel-based designs have an excellent capture envelope due to the nature of the funnel shape. However, they are bulky systems to install and are not adaptable to support multiple types of AUVs. For example, the REMUS docking station (see Fig. 1) is only capable

0364-9059 © 2018 IEEE. Personal use is permitted, but republication/redistribution requires IEEE permission.
See http://www.ieee.org/publications_standards/publications/rights/index.html for more information.

This article has been accepted for inclusion in a future issue of this journal. Content is final as presented, with the exception of pagination.

TABLE I
EXISTING DOCKING STATION SOLUTIONS FOR AUVS

Docking System	Capture Envelope	Size	Adaptability
Cone shaped funnel[12], [13]	Excellent	Poor	Poor
Pole[11]	Moderate	Moderate	Moderate
Grappling[16]	Poor	Excellent	Poor
Stinger [2]	Poor	Excellent	Moderate
Hook[17]	Poor	Excellent	Moderate

of supporting the REMUS vehicle and cannot support other similar vehicles. Pole type docking systems involve a fixed vertical pole with a flat v-shaped latching mechanism on the nose of the AUV [11]. Once latched, the AUV is pushed into the docked position through motorized carriages on the docking station. Pole-based designs enable a large vertical capture area with a relatively small horizontal capture area. Pole docks have historically had problems with homing and maintaining the necessary vertical attitude [14].

More novel docking solutions have been experimented with including grappling type [16], stinger and puck [18], hook [17], and vertical cones [19]. These various solutions each have unique benefits and drawbacks. For example, large funnel shaped docks such as those used by REMUS [13] and Bluefin-21 [12] have a large capture envelope and, once docked, form a rigid coupling between dock and vehicle. Table I presents a review of existing underwater docking systems. Each of the docking systems is scored on three criteria: capture envelope, size, and adaptability. The core functionality of any docking station is a large enough capture envelope to support docking of AUVs. Larger capture envelopes enable less accurate (and less costly) sensors to be used as well as allows docking in more adverse conditions. Limiting factors in charging station deployments are the sizes of the station and the adaptability to a wide variety of AUVs. In Table I, larger capture areas, smaller docking components (both station and adapter), and support for a variety of vehicles is ideal.

Marine docking systems have not yet been explored as thoroughly as docking systems in other domains, such as between aerial vehicles and between space vehicles. These other domain systems can help inspire the next generation of marine docking systems to overcome the shortcomings of current systems. Table II presents a review of these docking concepts. Magnetic docking has been adopted in marine robotics and has been used successfully to dock small scale robots, such as the ANGELS and CoCoRo AUVs [20]. The passive alignment and lack of exposed moving parts simplifies alignment and maintenance. However, purely magnetic solutions quickly become unfeasible as vehicles scale upwards due to the large forces involved in maintaining a rigid connection. One additional docking mechanism design is the Androgynous Peripheral Docking System used on the International Space Station [22]. This system allows significant misalignment in all six degrees of freedom and ensures a positive locking of the vehicle to the station. The marine environment makes the complex moving parts required to achieve this docking system challenging due to biofouling concerns.

Transmission of power is particularly challenging in the marine environment. The two most common methods to transfer power are through stab connectors or inductive power transfer systems. Stab connectors involve physically penetrating a series of membrane layers, oil baths, wipers, and seals to ensure that the electrical contacts on a connector are free of water before making a connection. This approach means that once connected, stab connectors are equivalent to a direct electrical connection. Stab connectors are however very sensitive to misalignment, cannot support high cycle lives, and require significant force to connect [23], [24]. The main alternative to stab connectors is inductive power transfer. Inductive systems utilize magnetic resonance coupling between primary and secondary coils to transfer power [25], [26]. Inductive systems are in use for aerial, ground, and marine systems [24], [27]– [32].

Navigation during docking is typically broken into five stages en route, approach setup, approach, terminal homing, and capture [14]. The en route stage is when the vehicle navigates using long range sensors. Approach setup and approach are completed once the vehicle is within range of the docking sensors, such as ultrashort baseline systems. In these stages, the AUV sets itself up for either a direct approach or a more novel approach like a hybrid sliding approach [33]. During the final few meters the terminal homing stage involves the AUV using high accuracy, quickly updating sensor feedback to increase docking precision. Following impact, the capture stage involves the AUV continuing to thrust until docked. This paper focuses on the terminal homing and capture stages. Depending on the sensors chosen and conditions the range for near-field navigation can be up to 100 m [20]. The cross-track controller attempts to zero the cross-track error and drive the AUV toward the docking station. Many different approaches to controlling the docking stage have been completed with the various limited sensor options available to AUVs including a one-camera, one-light approach [34], visual SLAM [35], stereo vision [36], magnetic guidance [37], and others [14], [33], [38]. Despite these efforts, the limited sensor and actuator fidelity available in the marine environment means that failed docking attempts are expected. Due to this, the docking protocol must be able to automatically recognize a failed docking attempt and reinitialize the docking routine.

III. PROPOSED DOCKING SOLUTION

A new docking solution that is capable of excelling in capture area, size, and adaptability is needed to bring AUV docking from limited mission specific deployments into common usage. With this in mind, the authors have developed a novel docking design that is low-cost, features a large capture envelope, is adaptable to a wide range of vehicle sizes, and is able to be installed in a wide variety of situations. The docking solution consists of two distinct pieces: a fixed docking station and a docking adapter mounted on top of the AUV.

The docking station (see Fig. 2) is designed to be a scalable solution for different class vehicles. The station is a rigid frame consisting of several key design features.

1) A simplified flat funnel is mounted at a sweep angle (Λ) and serve to guide the AUV into the dock along the horizontal plane.
2) A ramp (mounted at angle Ψ) pulls the AUV up into the docking station after it has been guided toward the dock.
3) Once the AUV is in the dock, a switchable magnet latches the vehicle into the station.
4) Power and data are transferred wirelessly through an inductive power module. The unique docking station design has no exposed moving parts to reduce problems caused due to biofouling.

The docking adapter (see Fig. 3) is designed to be mounted on top of traditional torpedo shaped AUVs as a drop-in replacement for the existing antenna mast. The adapter is capable of being mounted on different diameter vehicles though custom designed bumpers, no other modification is required. Key features of the docking adapter design are the guide planes, wireless power module, and magnetic coupling. The mast on the docking adapter is designed to slide along the docking station simplified funnel to bring the vehicle into the dock. Once in the dock, the guide planes slide up the ramp to bring the vehicle up into the station. The mast can serve dual purpose as antennas (Iridium, GPS, WiFi, etc.) can be installed if desired. The docking adapter impacts

This article has been accepted for inclusion in a future issue of this journal. Content is final as presented, with the exception of pagination.

TABLE II
EXISTING DOCKING CONCEPTS FROM OTHER DOMAINS AND THEIR APPLICABILITY TO MARINE SYSTEMS

Docking System	Adaptable Idea to Marine
Electromagnetic[20]	Enables passive alignment and disconnection
Magnetic[20]	Enables passive alignment
Probe and Drogue[21]	Mobile refueling
Androgynous Peripheral Docking Systems[22]	Control methodology

TABLE III
EXPERIMENTAL SPEED CALIBRATION OF BLUEFIN SANDSHARK AUV WITH AND WITHOUT DOCKING ADAPTER

Speed (RPM)	With adapter (m/s)	Without adapter (m/s)	Percentage difference
550	0.61	0.66	-7.9%
650	0.75	0.80	-6.0%
750	0.89	0.93	-4.7%
850	1.03	1.07	-3.7%

Speeds with adapter are from timed pool speed runs, speeds without adapter are from vehicle speed estimate.

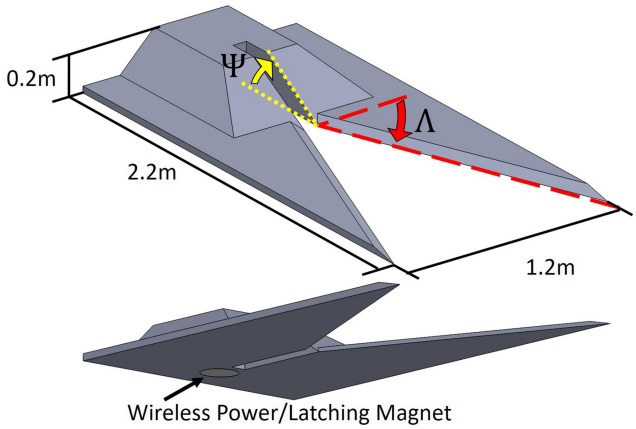

Fig. 2. Docking station is a scalable solution to allow docking with a variety of AUVs. It contains the docking mechanisms along with the power and data transfer modules required to support an extended AUV mission. This paper explores the optimization of two angles, sweep (Λ), and ramp (Ψ) with regards to capture envelope and maximum contact force. All major electronic components including the wireless power/data links and the latching magnet are located underneath the raised area of the docking station.

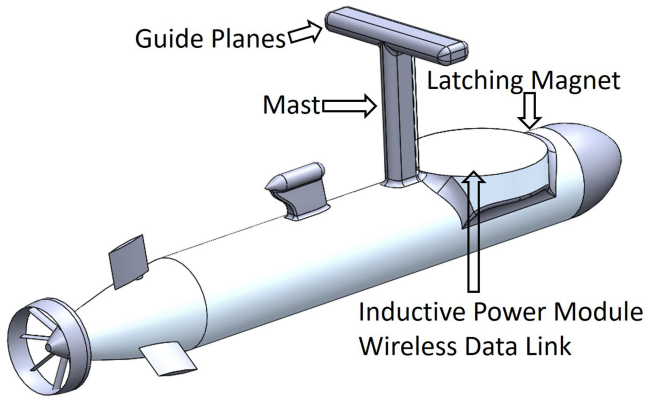

Fig. 3. Docking adapter is a drop-in replacement for a traditional AUV antenna mast. It contains the required power and data transfer modules as well as the docking mechanisms and can be scaled to a variety of AUV classes. Presented here is the docking adapter for a Bluefin SandShark. The design can be attached to other torpedo-shaped AUVs with minimal modification to the AUV.

overall vehicle performance slightly, in initial experimental testing this has been measured at approximately 4%, as given in Table III.

Fig. 4 shows a flowchart of the docking protocol in the docking stage. The docking process begins when the AUV is required to charge, at this point the AUV navigates to the neighborhood of the docking station using medium to long range navigation such as ultrashort baseline and dead reckoning. Once in range of the docking sensors (up to 100 m depending on sensors and conditions [14]), the AUV begins the docking procedure. The flight path represents the desired trajectory to enable docking. The docking adapter then impacts the docking station and guides the vehicle into the station. If the docking attempt fails, the AUV will fly around to the initial position for the docking procedure and reattempt. The noncontact latching magnet is triggered on the docking station once docking is successful, locking the vehicle into the power transfer location. Power and data are then transferred until the AUV is ready to go on mission again. To return to mission, the latching magnet is switched OFF and the AUV reverses to a safe distance before starting its new mission. This homing process is only required to control the horizontal plane motion of the AUV. In the vertical plane, the docking station depth is known by the AUV before docking. The AUV will be able to accurately achieve the correct depth to dock using pressure and altimeter measurements, typical expected depth performance is within a few centimeters of the depth target [39].

Presented in this paper is the docking station and docking adapter for a Dolphin II AUV [40], [41] and a Bluefin SandShark. The Dolphin II has a 0.2-m diameter and is 2.47 m long. The Bluefin SandShark has a 0.12-m diameter and is 1 m long. The docking station and docking adapter are able to be implemented for almost any AUV as the only vehicle requirement is an area to mount the docking adapter and a hull penetration to allow power and data to flow between the adapter and the AUV main system. Experimental validation will be completed using a Bluefin SandShark [42] and an OceanServer Iver3 [43], which are available to the authors. Power transfer between the vehicles can be accomplished with many different methods, for the purposes of this paper a WFS Seatooth Connect will be modeled that is capable of trans-

This article has been accepted for inclusion in a future issue of this journal. Content is final as presented, with the exception of pagination.

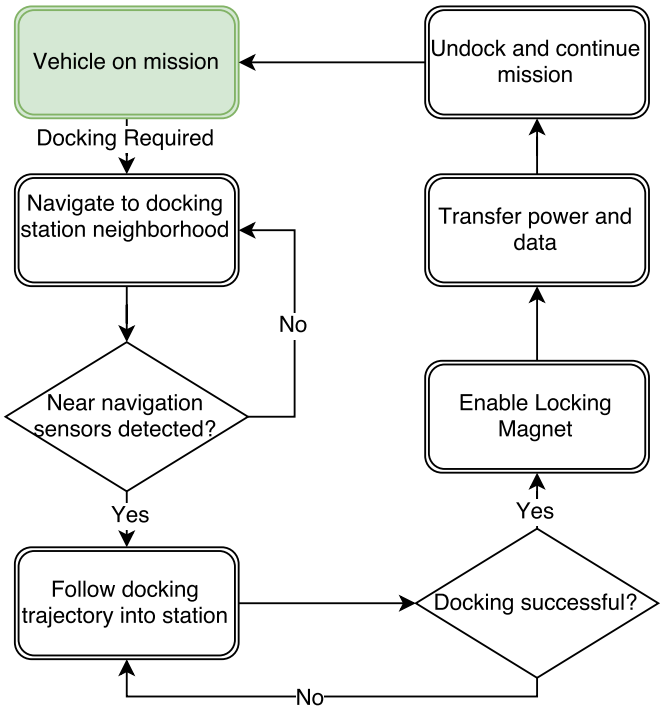

Fig. 4. During docking the AUV will attempt docking until docking is successful. It is expected that occasional failed docking attempts will occur due to low fidelity control and sensing during the docking maneuver.

mitting 50 W wirelessly. Once performance is validated, the Seatooth Connect can scale up to 3 kW. The scaled up WFS system is equivalent or higher than recent power ratings for other docking systems [44]. Docking navigation will be accomplished through a one-camera, one-light setup as in [34]. Other sensor setups will be experimented with following initial validation of the docking system.

IV. Dynamic Modeling

The dynamic model used in this paper is based on the work completed by [40] and [45] and is generalized for traditional AUVs. Consistent with this prior work, some assumptions are required to simplify the hydrodynamic and impact models. These include the following.

1) Both AUV and docking station are considered rigid bodies with small deformations in the impact region.
2) The docking station is fully fixed.
3) The AUV is trimmed perfectly neutral with a small purely vertical distance between center of mass and center of buoyancy to self-right the vehicle.
4) The thruster is assumed to be a purely forward force.
5) The impact process is short and can be modeled as a spring-damper as no permanent deformation considered.
6) Environmental disturbances are ignored.

In accordance with [46], both body-fixed and earth-fixed coordinate frames are defined in Fig. 5. The body frame is centered on the center of buoyancy of the AUV. The earth frame is chosen to be located on the dock such that when successful docking occurs, the two frames coincide.

To effectively model the AUV during the docking process two separate models are required. The hydrodynamic model represents the vehicle traveling through water and includes the various drag terms, added mass, and other effects. The impact model represents the contact forces generated by the collision between the docking adapter and the

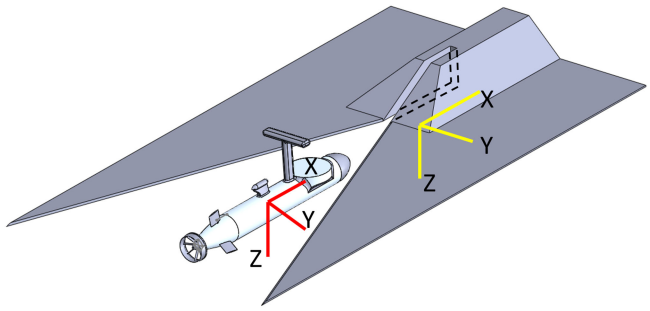

Fig. 5. Body-fixed frame (red) is located at the center of buoyancy of the AUV and the earth-fixed frame (yellow) is located on the docking station such that when successful docking occurs, the two frames coincide.

docking station. It models both the normal force from impact as well as the associated friction.

A. Hydrodynamic Model

Vehicle hydrodynamics are separated into viscous and inviscid terms. The viscous forces (f_v) and moments (m_v) are expressed as follows:

$$\boldsymbol{f}_v = \begin{pmatrix} X_v \\ Y_v \\ Z_v \end{pmatrix}$$
$$\boldsymbol{m}_v = \begin{pmatrix} K_v \\ M_v \\ N_v \end{pmatrix}. \quad (1)$$

To nondimensionalize the forces and moments, $0.5\rho V^2 L^2$ and $0.5\rho V^2 L^3$ are used as follows when V is the magnitude of velocity and L is the characteristic length:

$$X'_v = \frac{X_v}{0.5\rho V^2 L^2}, \quad Y'_v = \frac{Y_v}{0.5\rho V^2 L^2}, \quad Z'_v = \frac{Z_v}{0.5\rho V^2 L^2}$$
$$K'_v = \frac{K_v}{0.5\rho V^2 L^3}, \quad M'_v = \frac{M_v}{0.5\rho V^2 L^3}, \quad N'_v = \frac{N_v}{0.5\rho V^2 L^3}. \quad (2)$$

According to [47] and [48], the nondimensional quantities can be calculated following to

$$X'_v = C_X(\alpha) = C_X^0 + C_X^{\alpha_1}\alpha + C_X^{\alpha_2}\alpha^2 + C_X^{\alpha_3}\alpha^3 + C_X^{\alpha_4}\alpha^4$$
$$K'_v = C_K(\beta, \bar{p}, \bar{r}, \delta_r) = C_K^{\beta}\beta + C_K^{\bar{p}}\bar{p} + C_K^{\bar{r}}\bar{r} + C_K^{\delta_r}\delta_r$$
$$Y'_v = C_Y(\beta, \bar{p}, \bar{r}, \delta_r) = C_Y^{\beta}\beta + C_Y^{\bar{p}}\bar{p} + C_Y^{\bar{r}}\bar{r} + C_Y^{\delta_r}\delta_r$$
$$M'_v = C_M(\alpha, \bar{q}, \delta_e) = C_M^{\alpha}\alpha + C_Z^{\bar{q}}\bar{q} + C_M^{\delta_e}\delta_e$$
$$Z'_v = C_Z(\alpha, \bar{q}, \delta_e) = C_Z^{\alpha}\alpha + C_Z^{\bar{q}}\bar{q} + C_Z^{\delta_e}\delta_e$$
$$N'_v = C_N(\beta, \bar{p}, \bar{r}, \delta_r) = C_N^{\beta}\beta + C_N^{\bar{p}}\bar{p} + C_N^{\bar{r}}\bar{r} + C_N^{\delta_r}\delta_r. \quad (3)$$

Where α and β are angle of attack and sideslip angles, δ_r and δ_e are rudder and elevator angles, and the angular velocities are nondimensionalized according to $\bar{p} = pL/V$, $\bar{q} = qL/V$, and $\bar{r} = rL/V$. The viscous coefficients for the Dolphin II are provided in [40]

Inviscid hydrodynamic effects are represented by the generalized added inertia matrix following SNAME notation [46]. Due to vehicle symmetry and effective terms, the generalized added inertia matrix can

This article has been accepted for inclusion in a future issue of this journal. Content is final as presented, with the exception of pagination.

TABLE IV
HYDRODYNAMIC PARAMETERS FOR BLUEFIN SANDSHARK WITH CUSTOM DOCKING ADAPTER

Notation	Value $(\cdot 10^{-3})$	Notation	Value $(\cdot 10^{-3})$
$C_X^{\alpha^0}$	-8.8	C_K^{β}	-2.6605
$C_X^{\alpha^1}$	2.2	$C_K^{\bar{p}}$	-1.9985
$C_X^{\alpha^2}$	8.7	$C_K^{\bar{p}}$	0.1182
$C_X^{\alpha^3}$	-43.8	$C_K^{\delta_r}$	-0.1936
$C_X^{\alpha^4}$	-29.7	C_M^{α}	-24.895
C_Y^{β}	-91.036	$C_M^{\bar{q}}$	-1.2761
$C_Y^{\bar{p}}$	-1.6793	$C_M^{\delta_e}$	0.1260
$C_Y^{\bar{r}}$	1.5561	C_N^{β}	38.469
$C_Y^{\delta_r}$	-4.8062	$C_N^{\bar{p}}$	0.7254
C_Z^{α}	-50.339	$C_N^{\bar{r}}$	-0.9780
$C_Z^{\bar{q}}$	-2.3061	$C_N^{\delta_r}$	0.1332
$C_Z^{\delta_e}$	9.1536		

be represented as

$$\mathbf{M}_f = \begin{pmatrix} \mathbf{M_f} & \mathbf{C}_f^T \\ \mathbf{C}_f & \mathbf{J}_f \end{pmatrix} = -\begin{pmatrix} X_{\dot{u}} & 0 & 0 & 0 & 0 & 0 \\ 0 & Y_{\dot{v}} & 0 & 0 & 0 & Y_{\dot{r}} \\ 0 & 0 & Z_{\dot{w}} & 0 & Z_{\dot{q}} & 0 \\ 0 & 0 & 0 & K_{\dot{p}} & 0 & 0 \\ 0 & 0 & M_{\dot{w}} & 0 & M_{\dot{q}} & 0 \\ 0 & N_{\dot{v}} & 0 & 0 & 0 & N_{\dot{r}} \end{pmatrix}. \tag{4}$$

The submatrices $\mathbf{M}_f$, $\mathbf{C}_f$, and $\mathbf{J}_f$ represent the added mass, hydrodynamic coupling, and added inertia, respectively

Forces and moments due to fluid inertia can then be described as in [49]

$$\begin{bmatrix} \mathbf{f_i} \\ \mathbf{m}_i \end{bmatrix} = -\mathbf{M}_f \begin{bmatrix} \dot{\mathbf{v}}_1 \\ \dot{\mathbf{v}}_2 \end{bmatrix}. \tag{5}$$

To nondimensionalize the inviscid forces and moments $0.5\rho L^3$, $0.5\rho L^4$, and $0.5\rho L^5$ were selected

$$\begin{aligned} X'_{\dot{u}} &= \frac{X_{\dot{u}}}{0.5\rho L^3} & K'_{\dot{p}} &= \frac{K_{\dot{p}}}{0.5\rho L^5} \\ Y'_{\dot{v}} &= \frac{Y_{\dot{v}}}{0.5\rho L^3} & M'_{\dot{q}} &= \frac{M_{\dot{q}}}{0.5\rho L^5} \\ Z'_{\dot{w}} &= \frac{Z_{\dot{w}}}{0.5\rho L^3} & N'_{\dot{r}} &= \frac{N_{\dot{r}}}{0.5\rho L^5} \\ Y'_{\dot{r}} = N'_{\dot{v}} &= \frac{Y_{\dot{r}}}{0.5\rho L^4} & Z'_{\dot{q}} = M'_{\dot{w}} &= \frac{Z_{\dot{q}}}{0.5\rho L^4}. \end{aligned} \tag{6}$$

The total hydrodynamic forces and moments can be calculated by summing both the viscous and inviscid terms due to superposition.

Two vehicles were simulated to validate the scalability of the docking system to support a range of AUVs. The Dolphin II has hydrodynamic parameters available in [40]. Our experimental test vehicle, a Bluefin SandShark was also simulated using hydrodynamic parameters calculated in ANSYS Fluent. Coefficients for the SandShark are available in Tables IV and V.

TABLE V
INVISCID COEFFICIENTS A CUSTOMIZED BLUEFIN SANDSHARK WITH DOCKING ADAPTER

Notation	Value $(\cdot 10^{-3})$	Notation	Value $(\cdot 10^{-3})$
$X'_{\dot{u}}$	-10.2304	$N'_{\dot{r}}$	-7.4664
$Y'_{\dot{v}}$	-17.0604	$Y'_{\dot{r}}$	23.1156
$Z'_{\dot{w}}$	-8.7571	$Z'_{\dot{q}}$	-11.0542
$K'_{\dot{p}}$	-0.0052	$M'_{\dot{w}}$	-2.8780
$M'_{\dot{q}}$	-3.7747	$N'_{\dot{v}}$	5.6454

B. Impact Model

Modeling of the impact between AUV and docking station follows the approach in [40]. During the docking scenario, both normal and frictional forces play a significant role in docking success or failure. One way to model impacts is the following force-indentation model [50]

$$F = F_c(\delta) + F_v\left(\delta, \dot{\delta}\right) + F_p\left(\delta, \dot{\delta}\right). \tag{7}$$

where F_c, F_v, and F_p are the elastic, viscous damping, and dissipative parts of the impact force and δ, $\dot{\delta}$ are the penetration and penetration rate.

Due to the slow speeds involved and assuming no permanent deformation (the dock and AUV are not damaged during the docking maneuver), the plastic deformation term is negligible. This simplifies the impact model to a spring-damper model

$$F = k\delta^e + c\dot{\delta} \tag{8}$$

where k is contact stiffness and e, c are the force exponent and damping coefficient which are calculated in [40]. Modeling of friction can be completed using a Coulomb's law approach.

C. Simulation Setup

Dynamic modeling of the docking system was completed in a multibody physics and hydrodynamic motion control co-simulation environment. MSC ADAMS software performs the impact modeling and multibody physics as well as makes all the three-dimensional visualizations. MATLAB is used to model the system hydrodynamics and motion controller. Fig. 6 demonstrates the relationship between the two simulation tools.

Calculation of the hydrodynamic forces and moments is completed in the hydrodynamic model. The linear and angular positions, velocities, and accelerations are output from the multibody physics model and fed into the hydrodynamic equations. These equations calculate the resulting forces and moments, which are then fed back into the multibody physics model. The model then in turn calculates AUVs next position, velocity, and acceleration including any impacts. The ADAMS simulation tool models impact with the simplified impact model, shown as follows:

$$F = \begin{Bmatrix} 0 & q > q_0 \\ k(q_0 - q)^e - c_{\max}(dq/dt)\text{step}(q, q_0 - d, 1, q_0, 0) & q \le q_0 \end{Bmatrix}. \tag{9}$$

In the simplified model, q and q_0 represent the actual and original distances between colliding bodies, k is the contact stiffness, $c_{\max}$ is the maximum damping coefficient, e is the force exponent, and d is the penetration depth. Friction in ADAMS is modeled using a Coulomb's

This article has been accepted for inclusion in a future issue of this journal. Content is final as presented, with the exception of pagination.

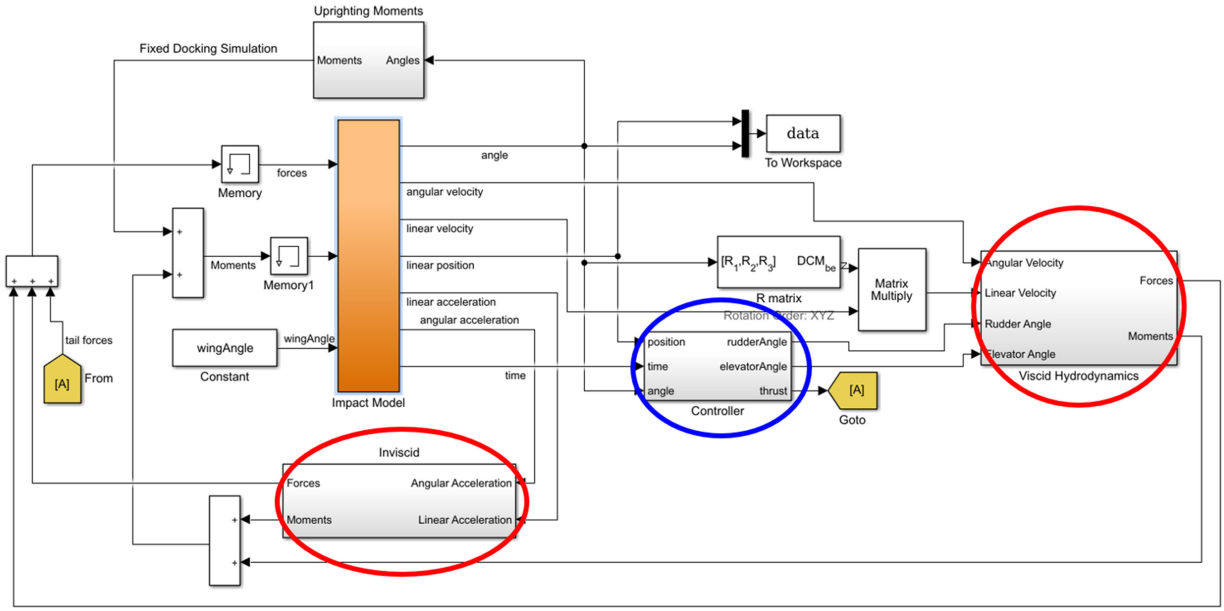

Fig. 6. Hydrodynamic motion control simulation calculates the vehicle hydrodynamics in the red circles, the vehicle controller in the blue circle, and connects to the multibody physics model in the orange block.

law approach combining static ($\mu_s = 0.08$) and dynamic ($\mu_d = 0.04$) friction.

This paper explores the effects of two design parameters (sweep angle Λ and ramp angle Ψ) and one control parameter (impact velocity) on the effective capture envelope and maximum impact force of the docking system when using a Dolphin II AUV. Numerical optimization of these three parameters was completed by simulating twenty different sweep angles (Λ) ranging from 22.5° to 67.5° while simultaneously varying the ramp angle (Ψ) between $30^\circ, 45^\circ,$ and 60°. The range of sweep angles includes all feasible solutions while maintaining a compact design and a sufficiently large capture envelope. During simulation, the three candidate ramp angles had a small impact on overall system performance so further refinement was deemed unnecessary. These 60 unique docking station configurations were each simulated with a 70 point, linearly spaced pattern to determine the feasible capture envelope. The 70 point pattern imitates the effect that disturbance and uncertainty will have during experimental deployments. Due to symmetry of the capture design, only impact locations with a $+Y$ measurement are explored and the results are mirrored to represent the full capture envelope. Attitude variation is not considered in this paper. Following convergence to optimal Λ and Ψ angles the simulation was then used to explore the effects of impact velocity on capture envelope and maximum impact force. The same 70 point scatter was completed for 20 impact velocities from 0.5 to 5 m/s. The optimization of Λ, Ψ, and impact velocity was completed with 5600 runs of the docking co-simulation and approximately 350 h of computation time. After optimization of the docking station and impact velocity using a Dolphin II AUV, the finalized docking system was evaluated using both a Bluefin SandShark and the Dolphin II. This evaluation was to validate the scalability of the docking station design to support a wide range of AUV sizes. The validation simulation involved docking of both vehicles with 5 cm linear spacing over the full capture envelope of the station. It required 105 runs and 8 h of computation time.

To navigate the vehicle toward the target impact location a Proportional Derivative (PD) controller was chosen that is used for the period of the simulation while the AUV approaches the docking station from its initial position 20 m away. The controller drives the AUV toward the docking station using the rudder and elevator angles while keeping the thrust constant. Feedback for this controller is the global YZ position. When the AUV approaches the docking station the controller switches to another controller that attempts to maintain pitch and yaw equal to

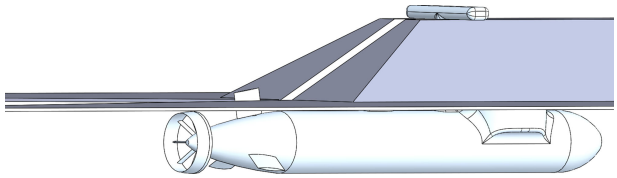

Fig. 7. When the vehicle is fully docked the mast and guide planes hold the AUV in place while the latching magnet firmly couples the vehicle into the docked position.

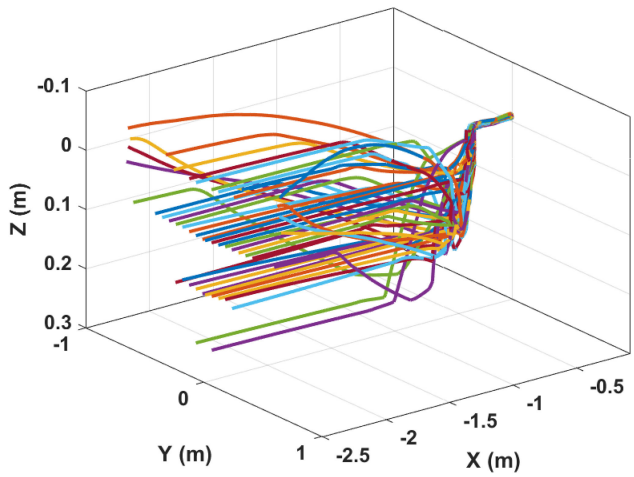

Fig. 8. Paths followed during successful docking attempts with a $3\pi/8$ sweep angle and 45° ramp angle. The docking pattern begins 2.5 m from the station with the 70 point scatter to imitate the effects of disturbances. Upon impact with the station the AUV begins sliding toward the receiver until it enters the dock located at (0, 0, 0).

This article has been accepted for inclusion in a future issue of this journal. Content is final as presented, with the exception of pagination.

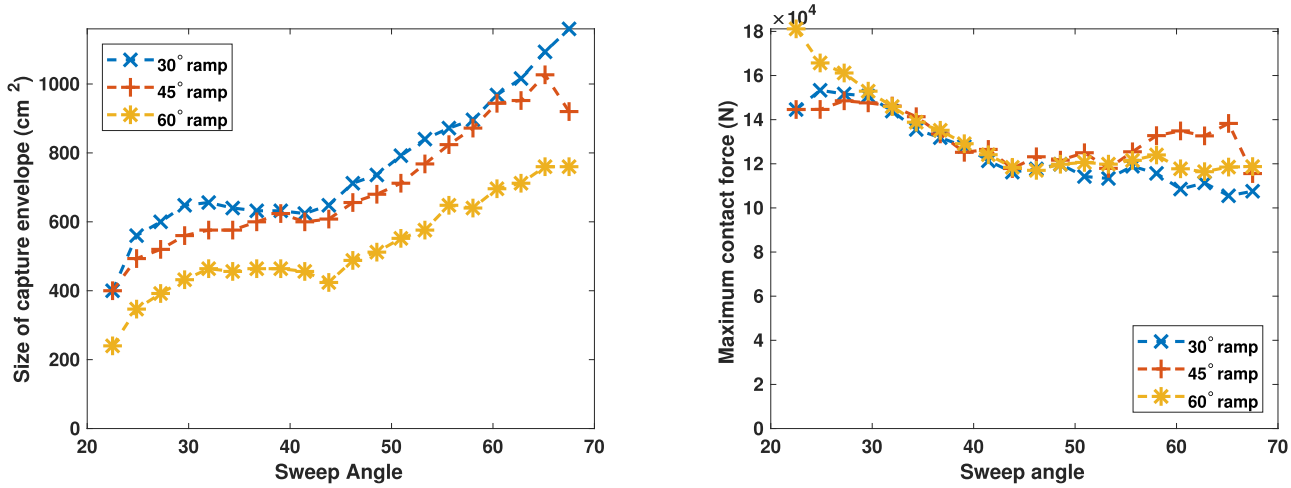

Fig. 9. Sweep and ramp angles both effect (a) capture envelope and (b) maximum impact force. Steeper sweep angles with flatter ramp angles lead to the largest capture envelopes with the smallest impact forces as the AUV is able slide along the guide pieces rather than bouncing off.

zero ($\theta = \psi = 0$). During experimental validation it is expected that more advanced controllers may be required.

V. Simulation Results

Numerical results from the ADAMS/MATLAB co-simulation can be used to optimize the design of the fixed docking station as well as aid controller development for docking. During the simulation runs, two design parameters (sweep angle Λ and ramp angle Ψ) were optimized with relation to the effective capture envelope and the maximum impact force based on the Dolphin II AUV. Docking is considered successful if the body-fixed frame and the earth-fixed frame are overlaid at the end of the simulation. In AUV terms this means that the docking adapter is inside of the receiver and the vehicle is lined up to support latching and power transfer, as shown in Fig. 7. Fig. 8 shows some of the successful docking approaches simulated. The figure shows the paths taken by the AUV during each of the successful tests over the 70 point scatter. While the simulation was completed from 20 m away, the trajectories presented here only include the final 2.5 m as this paper is focused on the final docking process. The docking paths initially slide downward and inward toward the receiver. Once at the entrance to the receiver, the path steeply climbs into the station which is located at (0, 0, 0).

The sweep angle (Λ), and ramp angle (Ψ) are two of the most critical design aspects in the novel docking design. In general, larger sweep angles lead to smoother docking with a wider covered area [see Fig. 9(a)]. The optimal sweep angle will result in a large successful capture area with a small maximum impact force [see Fig. 9(b)]. Based on the results, the ideal sweep angle is as large as possible and the ramp angle is as small as possible given sizing constraints. To achieve a similar width capture area to systems such the funnel in [40] with $\Lambda = 67.5^\circ$ the docking station will be 1.2 m wide, 2.2 m long, and 0.2 m tall (excluding seafloor supports). As the sweep angle approaches 90°, the required docking station length quickly becomes unreasonable. Similarly, if the ramp angle becomes too small, the length required to support the desired vertical capture envelope becomes unreasonable. To get a desired capture area we need to find a feasible combination of Λ and Ψ that fits within the station size constraints.

The maximum contact force experienced during either successful or failed docks is a critical design aspect. The maximum impact force dictates the required strength of components as both the AUV and docking station must survive repeated dockings without damage. The maximum contact force was measured in the ADAMS simulation for all the simulation runs and clustered based on sweep and ramp angle configuration. From these results, maximum impact force is dependent on the sweep angle while the ramp angle does not significantly affect impact force. Steeper sweeps lead to smaller maximum force, as shown in Fig. 9(b). The docking station design optimization was completed for full speed impacts of 3 m/s. High speed docking allows maximum control authority, but the very high impact force would require both AUV and docking system to be reinforced. The overall maximum impact force of 180 kN occurs during high speed docking maneuvers with an unoptimized docking station (small sweep and large ramp angles) and the large Dolphin II AUV. An optimized docking station reduces the maximum impact force to 120 kN when docking at high speeds.

Following optimization of the sweep and ramp angles, a further optimization was completed to explore the effect of impact velocity on docking envelope and maximum impact force. The 70 point scatter was simulated at 20 different impact velocities from 0.8 to 3.0 m/s. From the results (see Fig. 10), reducing the impact velocity not only significantly reduces maximum impact force to approximately 40 kN but also improves the capture area to the maximum size feasible with this design. This result indicates that if the docking adapter impacts the simplified funnel along its span, a successful docking will occur (see Fig. 11). Of note is the slight reduction in capture envelope at the lowest impact velocities in Fig. 10(a). This reduction is due to the constant thrust assumption, with the smallest thrust values the AUV is not able to overcome friction and enter the dock in a few cases.

The optimized docking station (see Fig. 2) has a sweep angle $\Lambda = 67.5^\circ$, a ramp angle $\Psi = 30^\circ$, and a target impact velocity of 1.0 m/s. This docking station is 2.2 m long, 1.2 m wide, and 0.2 m tall. During docking the maximum impact force that can be expected is 46 kN for a Dolphin II AUV. This docking station has an effective capture area of 0.35 m^2. This capture area is comparable to a 0.66 m diameter funnel dock. The flattened design of our docking station enables two docking stations to be packed into the same frontal area as the stations can be intertwined while on dock. This means that for the same ship volume, twice as much effective capture area can be deployed using this docking station than funnel-based designs reducing deployment costs when large numbers of stations are to be installed.

This article has been accepted for inclusion in a future issue of this journal. Content is final as presented, with the exception of pagination.

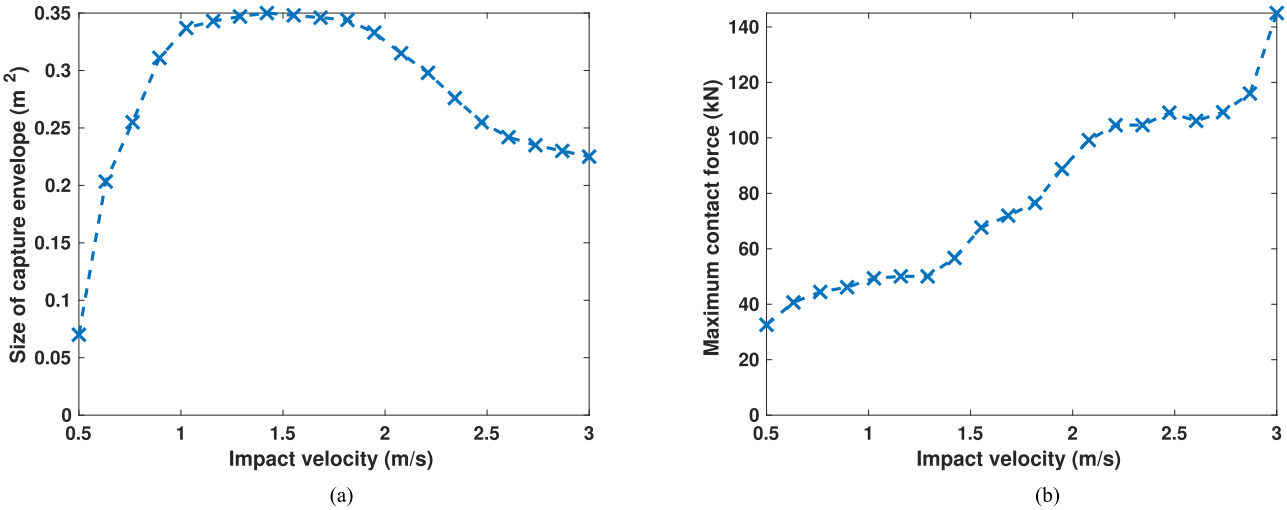

Fig. 10. Impact velocity has a significant effect on both (a) capture envelope and (b) maximum impact force. Slower impact speeds results in a sliding motion between the AUV and the docking station which leads to more successful docking and less impact force. Fast impact speeds results in a bouncing motion resulting in higher forces and more failed docking attempts.

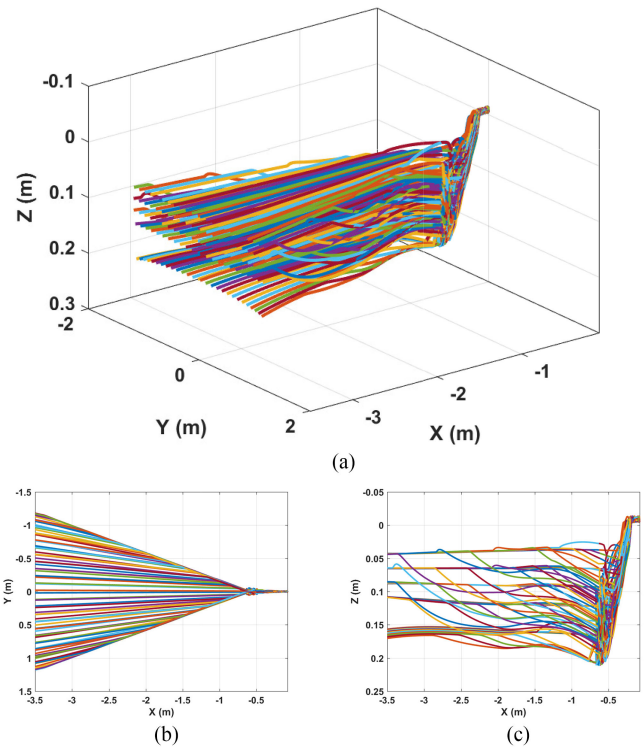

Fig. 11. At low speeds docking can occur anytime the docking adapter impacts the docking station regardless of location. (a) Isometric representation of the docking approach. (b) Top view of the docking approach showing the horizontal scatter and guiding into the docking station. (c) Side view showing the vertical scatter and guiding into the docking station.

The finalized docking station was then evaluated with both a Bluefin SandShark and the Dolphin II AUV at 5 cm linear spacing to determine the scalability of the common docking station for two very different vehicles. Out of the 135 tested trajectories, 49 were successful for the SandShark model and 47 were successful for the Dolphin II model. Some of the trajectories followed by the SandShark are shown in Fig. 12. The similarity between the SandShark and the Dolphin results while using identical docking stations and test scenarios

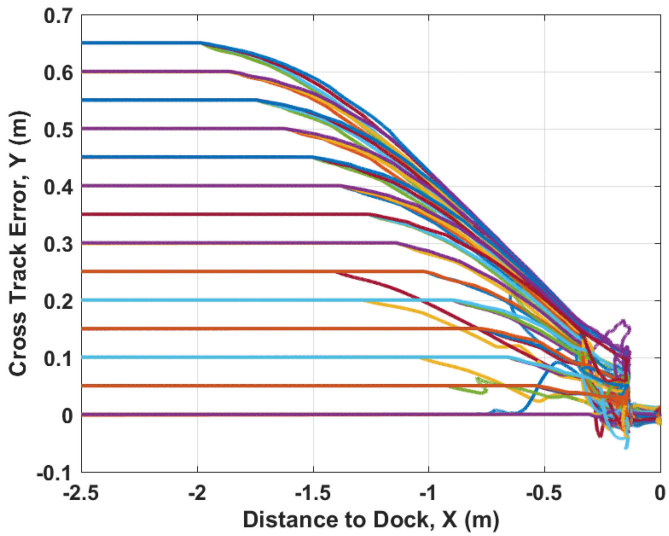

Fig. 12. Trajectories followed by the Bluefin SandShark during docking operations.

indicates that the docking station is capable of supporting a wide range of AUVs. Furthermore, it indicates that experimental validation with a Bluefin SandShark will be scalable to experimental validation with larger AUVs.

VI. Conclusion and Future Work

The novel docking station has been designed that reflects a current push for adaptable, small scale, long-duration underwater infrastructure. It features no exposed moving parts, enables a large capture envelope, and has an acceptable maximum impact force during docking. Furthermore, the design is small and lightweight resulting in rapid installation and low-cost operation. Key to the design is the adaptability to nearly any AUV. Due to the unique docking station design, one docking station can be used by different size classes of AUVs. This is accomplished by the docking adapter design (mounted atop the AUV) that is meant as a drop-in replacement for the traditional AUV antenna with additional charging components as well as the simplified funnel

This article has been accepted for inclusion in a future issue of this journal. Content is final as presented, with the exception of pagination.

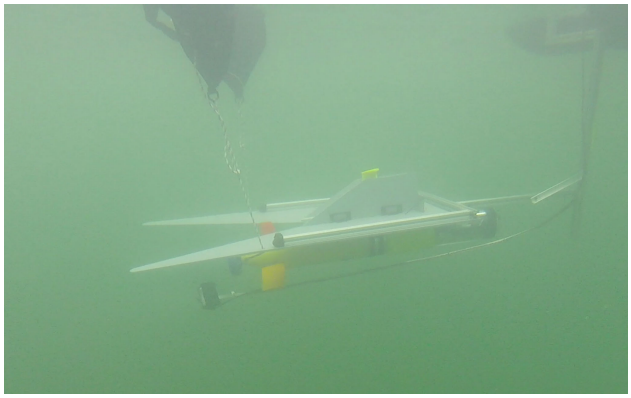

Fig. 13. Prototype Bluefin SandShark and docking station during initial open water validation in Lake Superior.

station design. The docking adapter is the only component that contacts the AUV and can be customized to different hulls quickly and at low cost.

The docking station design has been numerically optimized for two design parameters (sweep and ramp angles) and one control parameter (impact velocity). The results of this optimization shows that increasing sweep angle and decreasing ramp angle improves capture envelope and reduces maximum impact force. Furthermore, reduction of the impact velocity below the vehicle maximum improves maximum impact force and capture area. The simulation was completed using two AUV models, a large scale Dolphin II AUV and a small scale Bluefin SandShark with similar results.

With a now optimized docking station design, we will begin experimental validation using a customized Bluefin SandShark (see Fig. 13) and OceanServer Iver3. Material analysis will be completed before the prototyping stage to ensure functionality. Validation will begin with fixed trials in a controlled environment before moving to open water. Novel localization and control strategies will be experimentally validated starting with a one-camera, one-light approach. Stacked docking stations will be explored to support multiple AUVs simultaneously in a charging tree configuration. Furthermore, deployment and recovery of charging stations (and charging trees) will be completed. Going forward, one of the main motivations behind the novel docking station design is to create a mobile docking system similar to aerial refueling platforms. Further optimization of the design is required to minimize negative effects on the carrier vehicle to enable mobile charging. This mobile charging station will serve as charge carrying agent to a group of working robots and will be able to support extended AUV missions away from infrastructure.

ACKNOWLEDGMENT

The authors would like to thank S. J. Kang and Dr. H. Masoud for their assistance in determining the hydrodynamic parameters of the Bluefin SandShark with docking adapter.

REFERENCES

[1] "MBARI—Rates for vessels, vehicles, MARS, labor, test tank," Monterey Bay Aquarium Res. Inst., Moss Landing, CA, USA, 2017. [Online]. Available: http://www.mbari.org/at-sea/mars-ship-rates/

[2] T. Podder, M. Sibenac, and J. Bellingham, "AUV docking system for sustainable science missions," in *Proc. IEEE Int. Conf. Robot. Automat.*, Apr. 2004, vol. 5, pp. 4478–4484. [Online]. Available: https://doi.org/10.1109/ROBOT.2004.1302423

[3] V. Djapic and D. Nad, "Collaborative autonomous vehicle use in mine countermeasures," Nov. 2010. [Online]. Available: http://www.sea-technology.com/features/2010/1110/autonomous_vehicle.php

[4] S. Sariel, T. Balch, and N. Erdogan, "Naval mine countermeasure missions," *IEEE Robot. Automat. Mag.*, vol. 15, no. 1, pp. 45–52, Mar. 2008. [Online]. Available: https://doi.org/10.1109/M-RA.2007.914920

[5] G. Salavasidis, C. Harris, S. McPhail, A. B. Phillips, and E. Rogers, "Terrain aided navigation for long range AUV operations at arctic latitudes," in *Proc. IEEE/OES Auton. Underwater Veh.*, Nov. 2016, pp. 115–123. [Online]. Available: https://doi.org/10.1109/AUV.2016.7778658

[6] R. Lewis *et al.*, "Merlin—A decade of large AUV experience at memorial university of newfoundland," in *Proc. IEEE/OES Auton. Underwater Veh.*, Nov. 2016, pp. 222–229. [Online]. Available: https://doi.org/10.1109/AUV.2016.7778675

[7] R. B. Wynn *et al.*, "Autonomous underwater vehicles (AUVs): Their past, present and future contributions to the advancement of marine geoscience," *Mar. Geol.*, vol. 352, pp. 451–468, 2014. [Online]. Available: http://dx.doi.org/10.1016/j.margeo.2014.03.012

[8] A. Brighenti, L. Zugno, F. Mattiuzzo, and A. Sperandio, "Eurodocker-a universal docking-downloading recharging system for AUVs: Conceptual design results," in *Proc. MTS/IEEE OCEANS Conf.*, Sep. 1998, vol. 3, pp. 1463–1467. [Online]. Available: https://doi.org/10.1109/OCEANS.1998.726313

[9] S. Knepper, M. Niemeyer, R. Galletti, A. Brighenti, A. Bjerrum, and N. Andersen, "Eurodocker–a universal docking–downloading–recharging system for AUVs," *WIT Trans. Built Environ.*, vol. 53, pp. 1–9, 2001. [Online]. Available: https://doi.org/10.2495/MT010411

[10] T. B. Curtin, J. G. Bellingham, J. Catipovic, and D. Webb, "Autonomous oceanographic sampling networks," *Oceanography*, vol. 6, no. 3, pp. 86–94, 1993. [Online]. Available: http://www.jstor.org/stable/43924649

[11] H. Singh *et al.*, "Docking for an autonomous ocean sampling network," *IEEE J. Ocean. Eng.*, vol. 26, no. 4, pp. 498–514, Oct. 2001. [Online]. Available: https://doi.org/10.1109/48.972084

[12] R. S. McEwen, B. W. Hobson, L. McBride, and J. G. Bellingham, "Docking control system for a 54-cm-diameter (21-in) AUV," *IEEE J. Ocean. Eng.*, vol. 33, no. 4, pp. 550–562, Oct. 2008. [Online]. Available: https://doi.org/10.1109/JOE.2008.2005348

[13] R. Stokey *et al.*, "Enabling technologies for REMUS docking: An integral component of an autonomous ocean-sampling network," *IEEE J. Ocean. Eng.*, vol. 26, no. 4, pp. 487–497, Oct. 2001. [Online]. Available: https://doi.org/10.1109/48.972082

[14] J. G. Bellingham, *Autonomous Underwater Vehicle Docking*. New York, NY, USA: Springer, 2016, pp. 387–406. [Online]. Available: https://doi.org/10.1007/978-3-319-16649-0_16

[15] D. Pyle, R. Granger, B. Geoghegan, R. Lindman, and J. Smith, "Leveraging a large UUV platform with a docking station to enable forward basing and persistence for light weight AUVs," in *Proc. MTS/IEEE OCEANS Conf.*, Oct. 2012, pp. 1–8. [Online]. Available: https://doi.org/10.1109/OCEANS.2012.6404932

[16] P. Sotiropoulos, D. Grosset, G. Giannopoulos, and F. Casadei, "AUV docking system for existing underwater control panel," in *Proc. MTS/IEEE OCEANS Conf.*, May 2009, pp. 1–5. [Online]. Available: https://doi.org/10.1109/OCEANSE.2009.5278201

[17] T. Fukasawa, T. Noguchi, T. Kawasaki, and M. Baino, ""Marine bird", a new experimental AUV with underwater docking and recharging system," in *Proc. MTS/IEEE OCEANS Conf.*, Sep. 2003, vol. 4, pp. 2195–2200. [Online]. Available: https://doi.org/10.1109/OCEANS.2003.178242

[18] J. C. Lambiotte, R. Coulson, S. M. Smith, and E. An, "Results from mechanical docking tests of a Morpheus class AUV with a dock designed for an OEX class AUV," in *Proc. MTS/IEEE OCEANS Conf.*, Oct. 2002, vol. 1, pp. 260–265. [Online]. Available: https://doi.org/10.1109/OCEANS.2002.1193281

[19] Y. Ohta *et al.*, "A study of vehicle design to substantiate an underwater docking system for an AUV," in *Proc. 27th Int. Ocean Polar Eng. Conf.*, Jun. 2017.

[20] S. Mintchev, R. Ranzani, F. Fabiani, and C. Stefanini, "Towards docking for small scale underwater robots," *Auton. Robots*, vol. 38, no. 3, pp. 283–299, Mar. 2015. [Online]. Available: https://doi.org/10.1007/s10514-014-9410-3

[21] M. L. Fravolini, A. Ficola, G. Campa, M. R. Napolitano, and B. Seanor, "Modeling and control issues for autonomous aerial refueling for uavs using a probedrogue refueling system," *Aerospace Sci. Technol.*, vol. 8, no. 7, pp. 611–618, 2004. [Online]. Available: http://dx.doi.org/10.1016/j.ast.2004.06.006

This article has been accepted for inclusion in a future issue of this journal. Content is final as presented, with the exception of pagination.

[22] F. Maurelli, Y. Petillot, A. Mallios, S. Krupinski, R. Haraksim, and P. Sotiropoulos, "Investigation of portability of space docking techniques for autonomous underwater docking," in *Proc. MTS/IEEE OCEANS Conf.*, May 2009, pp. 1–9. [Online]. Available: https://doi.org/10.1109/OCEANSE.2009.5278115

[23] H. Painter and J. Flynn, "Current and future wet-mate connector technology developments for scientific seabed observatory applications," in *Proc. MTS/IEEE OCEANS Conf.*, Sep. 2006, pp. 1–6. [Online]. Available: https://doi.org/10.1109/OCEANS.2006.306829

[24] A. M. Bradley, M. D. Feezor, H. Singh, and F. Y. Sorrell, "Power systems for autonomous underwater vehicles," *IEEE J. Ocean. Eng.*, vol. 26, no. 4, pp. 526–538, Oct. 2001. [Online]. Available: https://doi.org/10.1109/48.972089

[25] W. Zhang, S. C. Wong, C. K. Tse, and Q. Chen, "Design for efficiency optimization and voltage controllability of series–series compensated inductive power transfer systems," *IEEE Trans. Power Electron.*, vol. 29, no. 1, pp. 191–200, Jan. 2014. [Online]. Available: https://doi.org/10.1109/TPEL.2013.2249112

[26] O. H. Stielau and G. A. Covic, "Design of loosely coupled inductive power transfer systems," in *Proc. Int. Conf. Power Syst. Technol.*, 2000, vol. 1, pp. 85–90. [Online]. Available: https://doi.org/10.1109/ICPST.2000.900036

[27] B. J. Heeres, D. W. Novotny, D. M. Divan, and R. D. Lorenz, "Contactless underwater power delivery," in *Proc. 25th Annu. IEEE Power Electron. Spec. Conf.*, Jun. 1994, vol. 1, pp. 418–423. [Online]. Available: https://doi.org/10.1109/PESC.1994.349700

[28] A. Askari, R. Stark, J. Curran, D. Rule, and K. Lin, "Underwater wireless power transfer," in *Proc. IEEE Wireless Power Transfer Conf.*, May 2015, pp. 1–4. [Online]. Available: https://doi.org/10.1109/WPT.2015.7139141

[29] J.-G. Shi, D.-J. Li, and C.-J. Yang, "Design and analysis of an underwater inductive coupling power transfer system for autonomous underwater vehicle docking applications," *J. Zhejiang Univ. Sci. C*, vol. 15, no. 1, pp. 51–62, 2014.

[30] B. Griffin and C. Detweiler, "Resonant wireless power transfer to ground sensors from a UAV," in *Proc. IEEE Int. Conf. Robot. Automat.*, May 2012, pp. 2660–2665. [Online]. Available: https://doi.org/10.1109/ICRA.2012.6225205

[31] L. Angrisani, G. d'Alessandro, M. D'Arco, V. Paciello, and A. Pietrosanto, "Autonomous recharge of drones through an induction based power transfer system," in *Proc. IEEE Int. Workshop Meas. Netw.*, Oct. 2015, pp. 1–6. [Online]. Available: https://doi.org/10.1109/IWMN.2015.7322968

[32] L. Angrisani, G. d'Alessandro, M. D'Arco, D. Accardo, and G. Fasano, "A contactless induction system for battery recharging of autonomous vehicles," in *Proc. IEEE Metrology Aerosp.*, May 2014, pp. 494–499. [Online]. Available: https://doi.org/10.1109/MetroAeroSpace.2014.6865975

[33] A. Sans-Muntadas, K. Y. Pettersen, E. Brekke, and V. F. Henriksen, "A hybrid approach to underwater docking of AUVs with cross-current," in *Proc. MTS/IEEE OCEANS Conf.*, Monterey, CA, USA, Sep. 2016, pp. 1–7. [Online]. Available: https://doi.org/10.1109/OCEANS.2016.7761213

[34] D. Li, T. Zhang, and C. Yang, "Terminal underwater docking of an autonomous underwater vehicle using one camera and one light," *Mar. Technol. Soc. J.*, vol. 50, no. 6, pp. 58–68, 2016. [Online]. Available: https://doi.org/10.4031/MTSJ.50.6.6

[35] H. J. Kang *et al.*, "Docking technique for manta-type UUV and its experimental studies in water tank environment," in *Proc. MTS/IEEE OCEANS Conf.*, Monterey, CA, USA, Sep. 2016, pp. 1–4. [Online]. Available: https://doi.org/10.1109/OCEANS.2016.7761384

[36] M. Myint, K. Yonemori, A. Yanou, K. N. Lwin, N. Mukada, and M. Minami, "Dual-eyes visual-based sea docking for sea bottom battery recharging," in *Proc. MTS/IEEE OCEANS Conf.*, Monterey, CA, USA, Sep. 2016, pp. 1–7. [Online]. Available: https://doi.org/10.1109/OCEANS.2016.7761319

[37] M. D. Feezor, F. Y. Sorrell, P. R. Blankinship, and J. G. Bellingham, "Autonomous underwater vehicle homing/docking via electromagnetic guidance," *IEEE J. Ocean. Eng.*, vol. 26, no. 4, pp. 515–521, Oct. 2001. [Online]. Available: https://doi.org/10.1109/48.972086

[38] C. Yang, S. Peng, S. Fan, S. Zhang, P. Wang, and Y. Chen, "Study on docking guidance algorithm for hybrid underwater glider in currents," *Ocean Eng.*, vol. 125, pp. 170–181, 2016. [Online]. Available: https://doi.org/10.1016/j.oceaneng.2016.08.002

[39] H. Singh *et al.*, "Imaging coral I: Imaging coral habitats with the seabed AUV," *Subsurface Sens. Technol. Appl.*, vol. 5, no. 1, pp. 25–42, Jan. 2004. [Online]. Available: https://doi.org/10.1023/B:SSTA.0000018445.25977.f3

[40] T. Zhang, D. Li, and C. Yang, "Study on impact process of AUV underwater docking with a cone-shaped dock," *Ocean Eng.*, vol. 130, pp. 176–187, 2017. [Online]. Available: https://doi.org/10.1016/j.oceaneng.2016.12.002

[41] M. Zhang, Y. Xu, B. Li, D. Wang, and W. Xu, "A modular autonomous underwater vehicle for environmental sampling: System design and preliminary experimental results," in *Proc. MTS/IEEE OCEANS Conf.*, Apr. 2014, pp. 1–5. [Online]. Available: https://doi.org/10.1109/OCEANS-TAIPEI.2014.6964495

[42] General Dynamics Mission Systems, "Bluefin SandShark autonomous underwater vehicle (AUV)," General Dyn. Mission Syst., Fairfax, VA, USA, 2017. [Online]. Available: https://gdmissionsystems.com/bluefinrobotics/vehicles-batteries-and-services/bluefin-sandshark

[43] OceanServer. "Iver AUV : New low cost AUV for coastal applications," 2017. [Online]. Available: http://www.iver-auv.com/products.html

[44] R. Lin, D. Li, T. Zhang, and M. Lin, "A non-contact docking system for charging and recovering autonomous underwater vehicle," *J. Mar. Sci. Technol.*, 2018, Sep. 2018. [Online]. Available: https://doi.org/10.1007/s00773-018-0595-6

[45] S. Peng, C. Yang, S. Fan, S. Zhang, P. Wang, and Y. Chen, "Hybrid underwater glider for underwater docking: Modeling and performance evaluation," *Mar. Technol. Soc. J.*, vol. 48, no. 6, pp. 112–124, 2014.

[46] T. I. Fossen, *Guidance and Control of Ocean Vehicles*. Hoboken, NJ, USA: Wiley, 1994.

[47] R. C. Nelson, *Flight Stability and Automatic Control*, vol. 2. New York, NY, USA: McGraw-Hill, 1998.

[48] B. N. Pamadi, *Performance, Stability, Dynamics, and Control of Airplanes*. Reston, VA, USA: AIAA, 2004.

[49] C. Brennen, "A review of added mass and fluid inertial forces." , Brennen (CE), Sierra Madre, CA, USA, Tech. Rep. CR 82.010, 1982.

[50] S. Faik and H. Witteman, "Modeling of impact dynamics: A literature survey," in *Proc. Int. ADAMS User Conf.*, vol. 80, 2000, pp. 1–11.

Brian R. Page received the M.S. degree in mechanical engineering from Michigan Technological University, Houghton, MI, USA, in 2016. He is currently working toward the Ph.D. degree in mechanical engineering with the School of Mechanical Engineering, Purdue University, West Lafayette, IN, USA.

His research interests include autonomous systems, controls, and mechanical design.

Nina Mahmoudian received the Ph.D. degree in aerospace engineering from Virginia Polytechnic and State University (Virginia Tech), Blacksburg, VA, USA, in 2009.

She is currently an Associate Professor of Mechanical Engineering with Purdue University, West Lafayette, IN, USA. She was the Lou and Herbert Wacker Associate Professor in Autonomous Mobile Systems with the Department of Mechanical Engineering–Engineering Mechanics, Michigan Technological University (Michigan Tech), Houghton, MI, USA. She is the founding Director of Nonlinear and Autonomous Systems Laboratory. Her research interests include robotics, energy autonomy, system design, dynamics and controls.

Dr. Mahmoudian was the recipient of the 2015 National Science Foundation CAREER Award and 2015 Office of Naval Research Young Investigator Program Award.